Multidisciplinary
SCIENTIFIC JOURNAL OF
MARITIME RESEARCH

University of Rijeka
Faculty of Maritime
Studies Rijeka

Multidisciplinarni
znanstveni časopis
POMORSTVO

Fuel mass flow variation in direct injection diesel engine – influence on the change of the main engine operating parameters

Vedran Mrzljak[1], Božica Žarković[1], Igor Poljak[2]

[1] University of Rijeka, Faculty of Engineering, Vukovarska 58, 51000 Rijeka, Croatia, e-mail: vmrzljak@riteh.hr, bozica.zarkovic@gmail.com
[2] Rožići 4/3, 51221 Kostrena, Croatia, e-mail: igor.poljak2@gmail.com

ABSTRACT

A change in the main operating parameters of a high speed turbocharged direct injection diesel engine MAN D0826 LOH15 during the fuel mass flow variation has been analyzed. On the basis of two measurement sets, on two different engine rotational speeds, performed with standard diesel fuel, several operating parameters have been calculated: engine torque, effective power, excess air ratio, specific effective fuel consumption and heat released per engine process. The calculated parameters are presented for a wide engine operating range. In addition to measurement sets, several important parameters have been measured. Additional measured parameters have been lubrication oil temperature and exhaust gas temperature before and after the turbocharger turbine. The presented engine operating parameters allow deep insight into the analyzed diesel engine process.

ARTICLE INFO

Preliminary communication
Received 14 October 2017
Accepted 4 December 2017

Key words:
Diesel engine
Fuel mass flow variation
Experimental analysis
Operating parameters

1 Introduction

Experimental measurements are the basis of internal combustion engines operating parameters analysis, [1] and [2], regardless of the engine type.

Numerous researchers are involved in the investigation of the diesel engines from the several points of view [3]. Experimental analysis of diesel engines will be impossible without proper engine management [4], troubleshooting and repairing processes [5]. Along with diesel engine measurements, numerical simulations have been developed in order to make easier, faster and much cheaper investigations of engine operating parameters [6].

Until now, several types of diesel engine numerical models have been developed. Each of them has its own advantages, specifics and disadvantages.

The earliest diesel engine numerical models were 0D (zero dimensional) models [7], which are very fast and reliable but are not able to predict emissions from diesel engines, at least not without certain approximations [8]. The improvement of 0D models was obtained with multizone models [9], which can predict diesel engine emissions, but the predictions are only general [10].

Multizone models were upgraded with QD (quasi dimensional) numerical models, which monitor each fuel spray inside the diesel engine cylinder by using the packages (control volumes). Such QD models were tested and validated in a wide range of diesel engines such as a high speed four-stroke diesel engine [11] and marine two-stroke diesel engine [12]. With regard to high speed, accuracy and precision, QD numerical models can also be used for predicting diesel engine operating parameters during the engine transient operations [13].

The most detailed diesel engine numerical models are CFD (Computational Fluid Dynamics) models [14]. These models provide the most accurate and the most precise predictions of the diesel engine operating parameters [15], but simulations have an extremely long time of calculation. CFD models are usually based on just one engine cylinder [16], because a simulation of the entire engine would be impossible without the use of supercomputers. As they are the most detailed, CFD simulations requires assuming certain operating parameters during the calculation start. Those assumed operating parameters are difficult or impossible to measure on a real diesel engine.

In order to determine the accuracy and precision of each model, they must necessarily be validated in several different measured operating points of the diesel engine. Therefore, experimental measurements are inevitable, even nowadays.

To improve engine operating parameters and reduce emissions, scientists are intensively involved in implementing combustion of alternative fuels in the existing diesel engines. Some analysis of the alternative fuel usage in diesel engines can be found in [17] and [18]. A review of alternative fuels for diesel engines can be found in [19] while in [20] a review of performance, combustion and emission characteristics of bio-diesel fueled diesel engines has been presented

Optimization of diesel engines can be performed in several ways [21]. The most used optimization methods are multi-objective optimization [22], multi response optimization [23], genetic algorithm optimization [24] and optimization by using Artificial Neural Networks (ANN) [25].

This paper aims to present the change in the main operating parameters of a high speed turbocharged direct injection diesel engine during the fuel mass flow variation. The operating parameters analysis has been based on two measurements set at two different engine rotational speeds. For each measured point, regardless of the measurement set, fuel and air mass flow have varied. Measurements have been obtained with a standard diesel fuel D2. The calculated parameters, which change is traced in each observed operation point, have been engine torque, effective power, excess air ratio, specific effective fuel consumption and heat released per engine process. Along with the presented measurement sets, measurement of additional engine operating parameters has been performed and those parameters have been the lubrication oil temperature and the exhaust gas temperatures before and after the turbocharger turbine. The presented operating parameters allow insight into a wide operating range of the analyzed engine.

2 Diesel engine specifications

The analyzed diesel engine is a high speed turbocharged engine with direct injection MAN D0826 LOH15. The main engine specifications and characteristics are presented in Table 1.

Table 1 Engine Specifications and Characteristics

Cylinder bore	108 mm
Cylinder stroke	125 mm
Crank radius	62.5 mm
Length of the connecting rod	187.2 mm
Nozzle diameter	0.23 mm
Number of nozzle holes	7
The total operating volume	6870 cm^3
Compression ratio	18
Number of cylinders	6
Peak effective power	160 kW

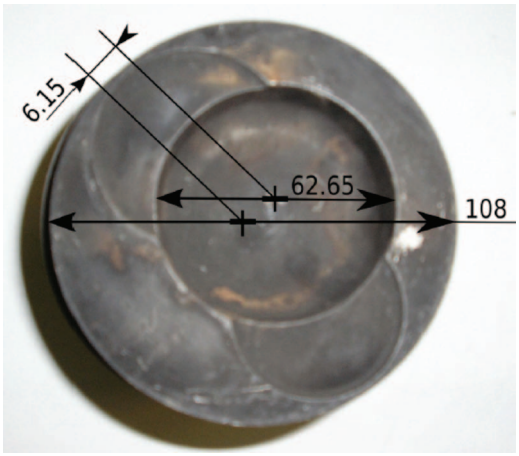

Figure 1 Engine Piston with Main Dimensions (in mm) and Eccentrically Positioned Hole

In order to maximize the suction and exhaust valve flow rate, the fuel injector is positioned eccentrically in relation to the cylinder symmetry axis and hence the hole in the piston head is positioned in the same way. As the fuel injection is performed in the vicinity of the top dead center, the fuel spray must have enough space for dispersion and mixing with the air, what is the primary purpose of a hole in the piston head, Figure 1.

3 Engine measuring equipment and measurement results

Engine measurement has been performed in the Laboratory for Internal Combustion Engines and Electromobility at the Faculty of Mechanical Engineering of the University of Ljubljana, Slovenia.

The measured engine has been connected to an eddy current brake Zöllner B-350AC, Figure 2. Measurements control has been secured with a control system KS ADAC/Tornado. Cylinder pressure has been measured with pressure sensor AVL GH12D, placed in an extra hole in the cylinder head. The cylinder pressure signal has been led to amplifier AVL MicroIFEM.

The piston top dead centre has been determined by a capacitive sensor COM Type 2653, and the crankshaft angle has been measured by crank angle encoder Kistler CAM UNIT Type 2613B with an accuracy of 0.1° crank angle.

The lubrication oil temperature has been measured with Greisinger GTF 401-Pt100 Immersion probe while the flue gas temperature at the turbocharger turbine inlet and outlet has been measured with two Greisinger GTF 900 Immersion probes.

A few measurement sets have been performed and two measurement sets, presented in Table 2 and Table 3 have been selected for the analysis. Each of the measurement set has almost a constant engine rotational speed (1500 rpm and 2400 rpm). In each measurement set, fuel and air mass flow continuously increases from measurement

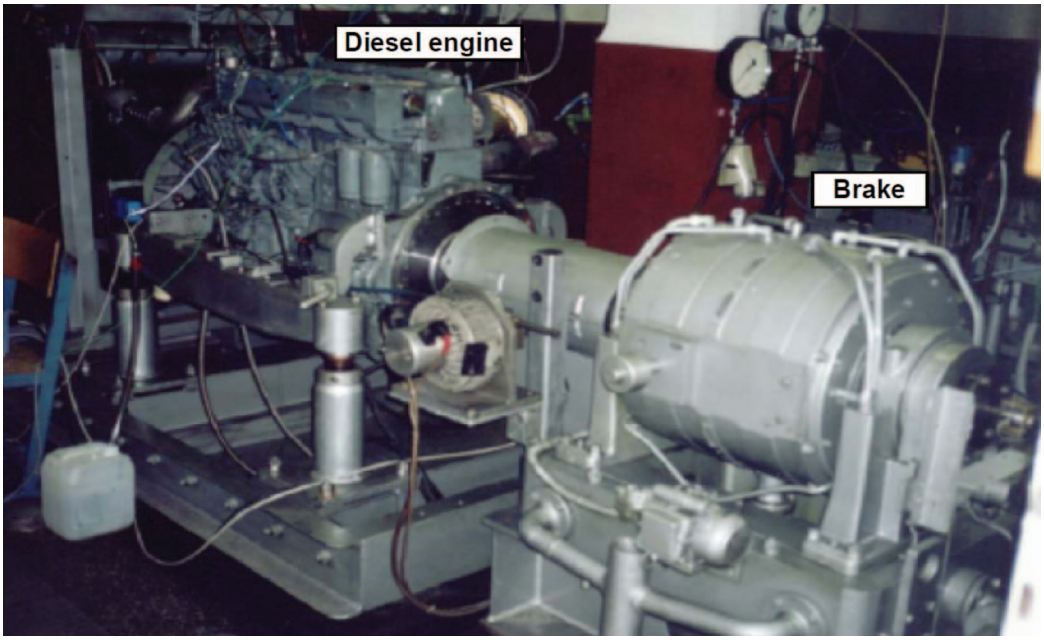

Figure 2 Diesel Engine MAN D0826 LOH15 Connected to Eddy Current Brake in the Laboratory

Table 2 Obtained Measurement Results – Set 1

Measurement No.	Fuel mass flow (kg/h)	Air mass flow (kg/s)	BMEP* (bar)	Brake reaction force (N)	Rotational speed (rpm)
1	9.743	0.09761	4.88	279.4	1501
2	13.977	0.10337	7.21	412.7	1498
3	18.673	0.12048	10.02	573.9	1501
4	23.358	0.13943	12.65	724.1	1500

* BMEP = Brake Medium Effective Pressure

Table 3 Obtained Measurement Results – Set 2

Measurement No.	Fuel mass flow (kg/h)	Air mass flow (kg/s)	BMEP* (bar)	Brake reaction force (N)	Rotational speed (rpm)
1	16.045	0.18775	4.13	236.5	2400
2	21.961	0.21650	6.40	366.4	2400
3	30.086	0.25726	8.99	514.5	2400
4	36.001	0.28798	10.60	606.6	2400

* BMEP = Brake Medium Effective Pressure

point 1 to 4. In this analysis, the impact of these two variables on the change of the other engine main operating parameters has been investigated.

4 Equations for calculating engine main operating parameters

Engine torque has been calculated by using the equation:

$$M = F \cdot R \tag{1}$$

where M (Nm) is the engine torque, F (N) is the brake reaction force and R (m) is the brake prong length at which end the reaction force is measured. For the used eddy current brake, the brake prong length amounts R = 0.955 m.

Engine effective power has been calculated according to the equation:

$$P_{ef} = \frac{M \cdot 2 \cdot \pi \cdot n}{60 \cdot 1000} \tag{2}$$

where P_{ef} (kW) is the effective power and n (rpm) is the engine rotational speed.

Excess air ratio has been calculated by using the equation:

$$\lambda = \frac{\dot{m}_a \cdot 3600}{\dot{m}_f \cdot L_{st}} \tag{3}$$

where λ (-) is the excess air ratio, $\dot{m}_a$ (kg/s) is the air mass flow, $\dot{m}_f$ (kg/h) is the fuel mass flow and L_{st} (-) is the stoichiometric air mass, which is dependable on the used fuel

properties. During measurements, the standard diesel fuel D2 has been used, which lower heating value (H_d) amounts to H_d = 42700 kJ/kg and the stoichiometric air mass for the used fuel amounts to L_{st} = 14.7.

Specific effective fuel consumption has been calculated according to the equation:

$$b_{ef} = \frac{\dot{m}_f \cdot 1000}{P_{ef}} \quad (4)$$

where b_{ef} (g/kWh) is the specific effective fuel consumption.

The heat released per engine process has been obtained according to the equation:

$$Q_{pp} = \frac{\dot{m}_f \cdot H_d}{n \cdot 60} \quad (5)$$

where Q_{pp} (kJ/proc.) is the heat released per engine process.

5 Change in engine operating parameters and discussion

For the lower observed engine rotational speed (1500 rpm – Set 1), an increase in the engine torque is much sharper than for the higher engine rotational speed (2400 rpm – Set 2), Figure 3. In the measurement Set 1, torque increases from 266.83 Nm up to 691.52 Nm, while in the measurement Set 2, torque increases from 225.86 Nm to 579.28 Nm.

Comparing both measurement sets, for the same fuel mass flow, engine torque in Set 1 is approximately two times higher than torque in Set 2. The change of engine torque, in each of the observed measurement sets is almost linear (engine torque linearly increases with the increase in the fuel mass flow).

For each of the engine rotational speeds, the increase in fuel mass flow is linearly followed by an increase in the engine effective power. In the measurement Set 1 at 1500 rpm, the investigated engine has developed a maximum effective power of 108.66 kW at a fuel mass flow of 23.358 kg/h, while in the measurement Set 2 at 2400 rpm, the engine has developed a maximum effective power of 145.56 kW at a fuel mass flow of 36.001 kg/h, Figure 4. The minimum achieved effective power in both measurement sets has been 41.93 kW – Set 1 and 56.76 kW – Set 2, for different fuel mass flows (9.743 kg/h – Set 1 and 16.045 kg/h – Set 2).

During the same fuel mass flow (range of fuel mass flow rates from 16 kg/h to 23.5 kg/h), as in Figure 4, it can be seen that the higher engine effective power has been developed at a lower rotational speed (1500 rpm – Set 1). According to equation (2), the reason for this fact is a much higher engine torque in Set 1 in comparison with the engine torque in Set 2, Figure 3. Therefore, it can be concluded that, for the observed engine, a greater impact on the change of the effective power has a change in the engine torque, when compared with the change in the torque with a change in the engine rotational speed.

In comparison with the gasoline engines, where the excess air ratio is strictly maintained at 1 (due to triple-action catalyst), the global excess air ratio in diesel engines has been always higher than 1. Only in certain zones within the diesel engine cylinder, the excess air ratio may be equal to 1, but these zones do not have a long life span and they have no major impact on the diesel engine global excess air ratio.

An increase in the fuel mass flow, in both measurement sets, reduces the value of the analyzed diesel engine global excess air ratio. According to equation (3), the increase in the fuel mass flow has a greater impact on the excess air ratio than the simultaneous increase in the air mass flow in both measurement sets. The maximum value of the excess air ratio in measurement Set 1 is 2.45 at the lowest observed fuel mass flow and it continuously decreas-

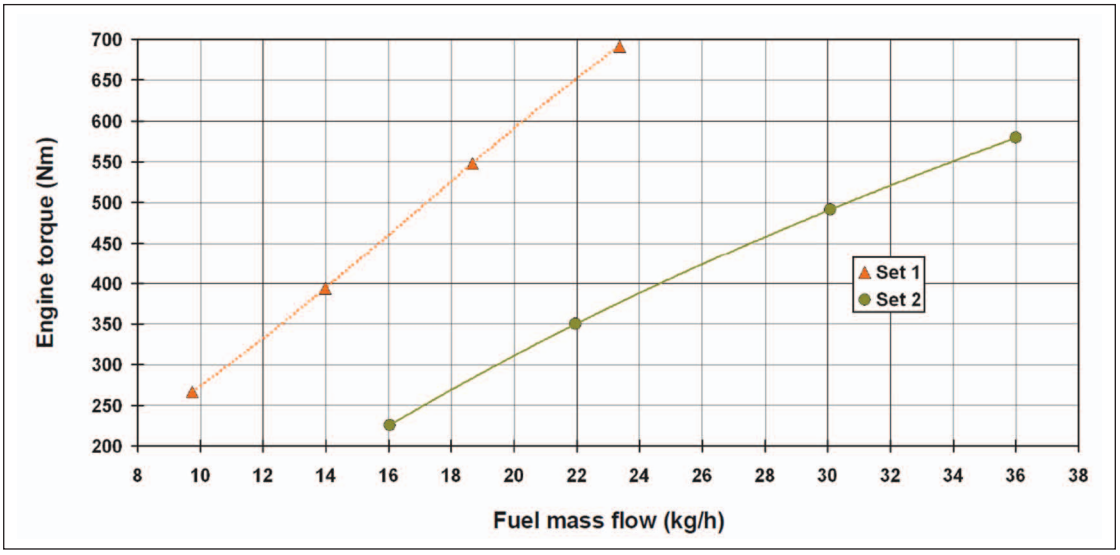

Figure 3 Engine Torque Change in Each Measurement Set

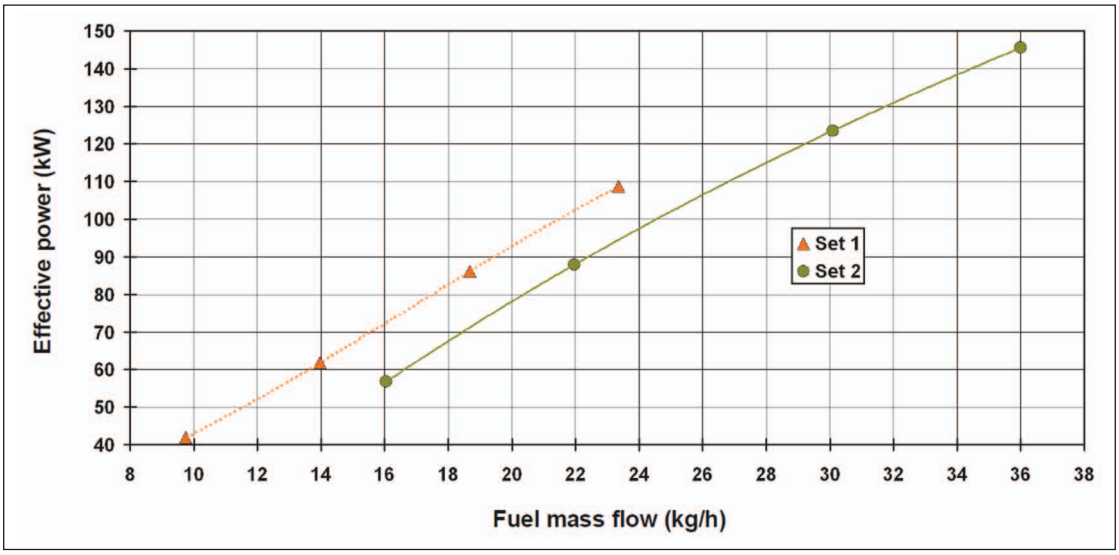

Figure 4 Engine Effective Power Change in Each Measurement Set

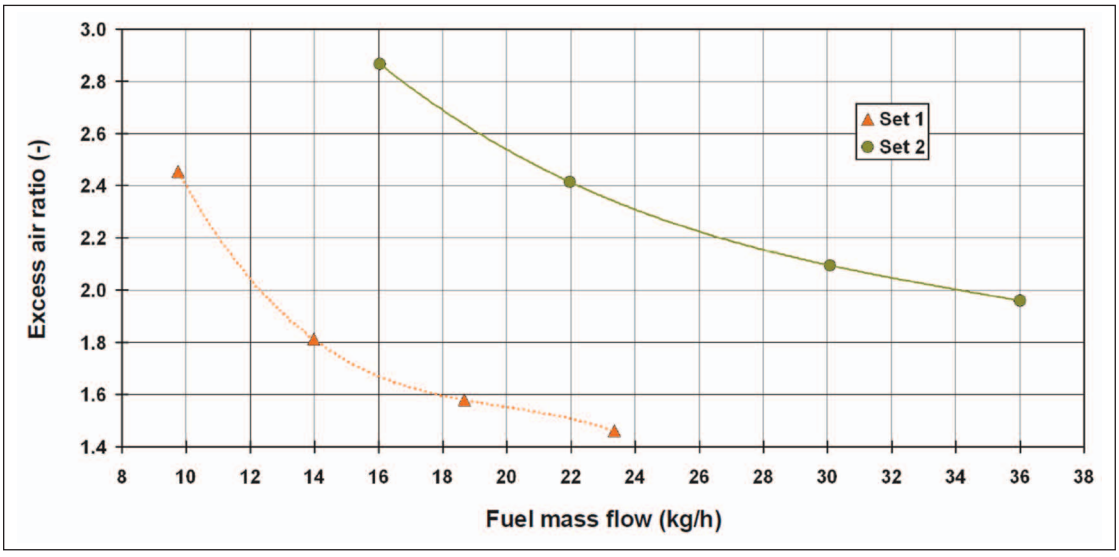

Figure 5 Excess Air Ratio Change in Each Engine Measurement Set

es with an increase in the fuel mass flow until a minimum value of 1.46 at a fuel mass flow of 23.358 kg/h, Figure 5. In measurement Set 2, the excess air ratio change during the increase in fuel mass flow is very similar to the measurement Set 1. The maximum value of the excess air ratio in Set 2 is 2.87 while the minimum value is 1.96.

For both diesel engine rotational speeds, as expected, the calculated global excess air ratio has a value significantly higher than 1 in all observed fuel mass flows.

For the most diesel engines which operate with standard diesel fuel as well as for the diesel engine analyzed in this paper, during the increase in the fuel mass flow, the specific effective fuel consumption firstly decreases up to the minimum value, after which a slight increase follows.

At the measurement Set 1, the maximum value of the specific effective fuel consumption amounts to 232.37 g/kWh, while in Set 2, the maximum value for the specific effective fuel consumption is 282.69 g/kWh, Figure 6. The highest specific effective fuel consumption values for both measurement sets has been calculated at the lowest fuel mass flow in each measurement set.

The minimum specific effective fuel consumption for the Set 1 is approximately 214 g/kWh, while in the Set 2 the minimum specific effective fuel consumption amounts to approximately 242 g/kWh.

It can be seen, from Figure 6, that for the same fuel mass flow a significantly lower specific effective fuel consumption has been obtained at the lower engine rotational speed (1500 rpm – Set 1) compared to the higher rotational speed (2400 rpm – Set 2).

The heat released per engine process, calculated at each engine operating point for both measurement sets by using equation (5), linearly increases during the increase in the fuel mass flow. In both measurement sets, trends of heat released per engine process growth are similar, with a sharper increase in measurement Set 1.

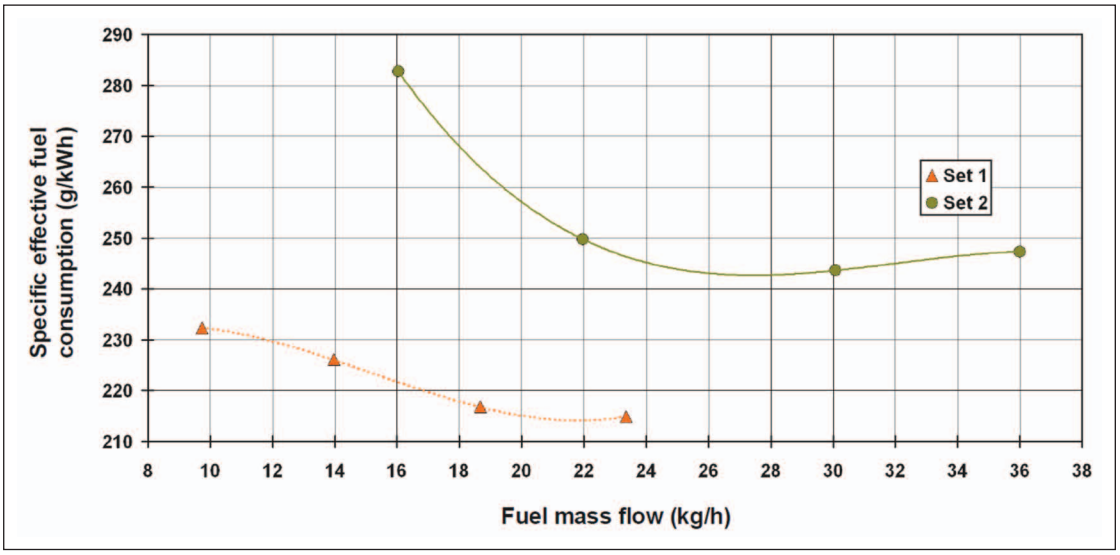

Figure 6 Engine Specific Effective Fuel Consumption Change in Each Measurement Set

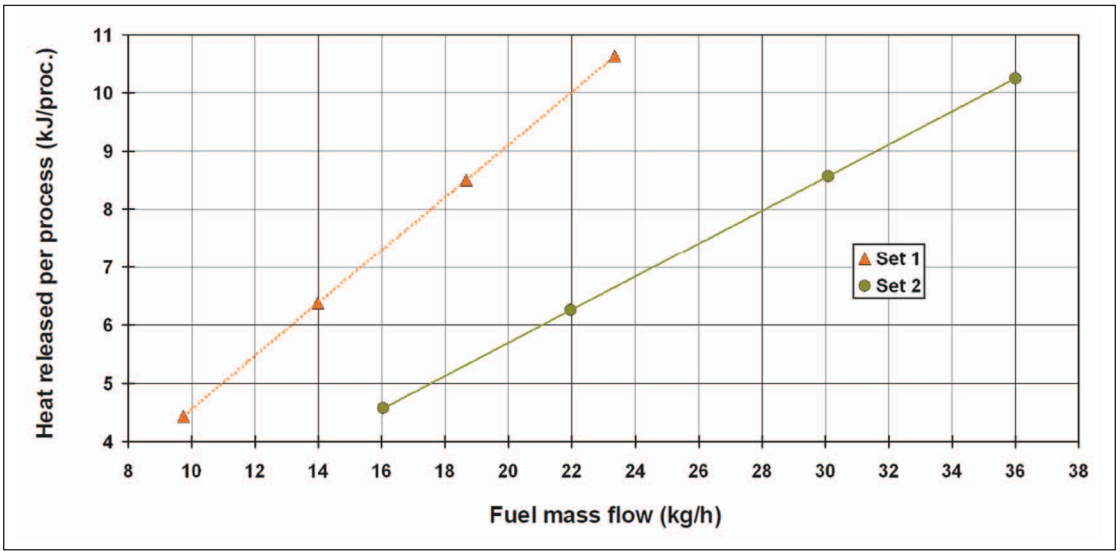

Figure 7 Heat Released per Engine Process Change in Each Measurement Set

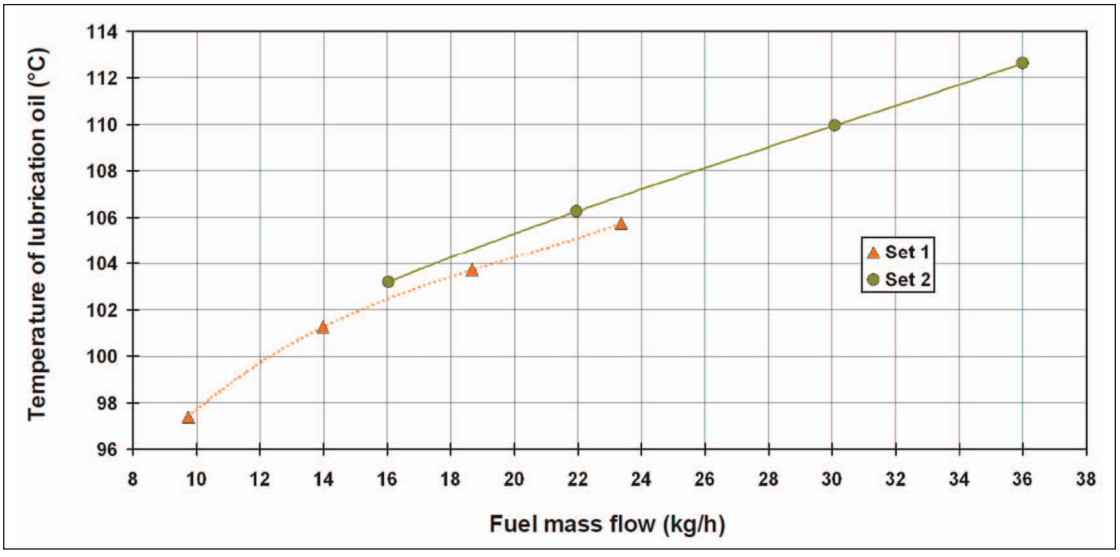

Figure 8 Lubrication Oil Temperature Change in Each Engine Measurement Set

The maximum and minimum values of the heat released per engine process are approximately the same for both measurement sets, Figure 7. In measurement Set 1, the heat released per engine process increases from 4.44 kJ/proc. at a fuel mass flow of 9.743 kg/h up to 10.64 kJ/proc. at a fuel mass flow of 23.358 kg/h. In Set 2, the heat released per engine process arises from 4.57 kJ/proc. at fuel mass flow of 16.045 kg/h up to 10.25 kJ/proc. at a fuel mass flow of 36.001 kg/h.

For the same fuel mass flow, a much higher heat released per engine process can be seen at lower engine rotational speed (Set 1) in comparison with higher rotational speed (Set 2), Figure 7.

The measured lubrication oil temperature continuously increases during the increase in fuel mass flow for both measurement sets of the analyzed engine, Figure 8. In the measurement Set 1, the lubrication oil temperature range is between 97.39 °C and 105.75 °C, while in the Set 2 the lubrication oil temperature range is between 103.20 °C and 112.63 °C. From Figure 8 it is apparent that the lubrication oil temperature change curve is not uniform in both measurement sets. In the measurement Set 2, the change of the lubrication oil temperature is linear, while in the Set 1 the curve significantly deviates from the linear change.

For the same fuel mass flow, a slightly higher lubrication oil temperature is observed in the measurement Set 2, at higher engine rotational speeds.

In neither of the measurement sets, the lubrication oil temperature has not reached the values near the oil temperature limit specified by the producer. Crossing the lubrication oil temperature limit would cause a loss of the expected oil characteristics and a problem in the engine operation could be expected.

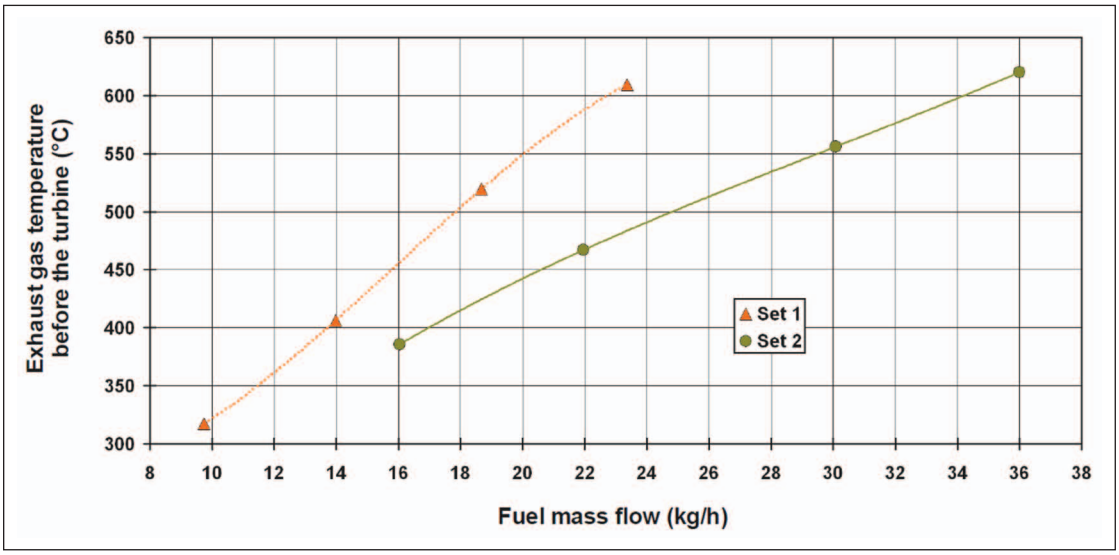

Figure 9 Exhaust Gas Temperature before the Turbine Change in Each Measurement Set

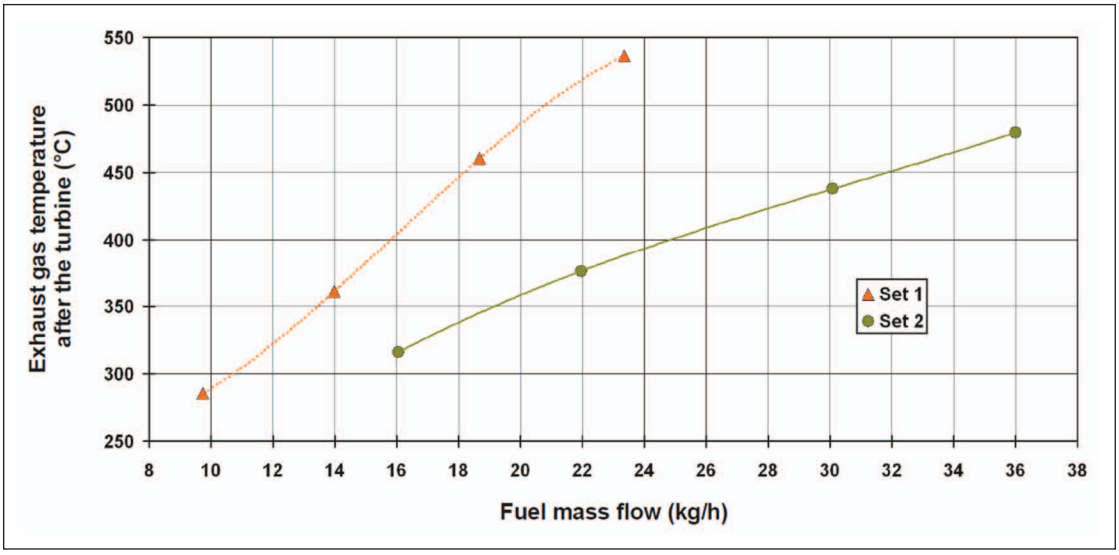

Figure 10 Exhaust Gas Temperature after the Turbine Change in Each Measurement Set

The analyzed engine has a turbocharger in order to increase the air pressure at the cylinder inlet and as a consequence save fuel. At the entrance into the turbine of the turbocharger, the exhaust gas has the highest temperature (and therefore the highest enthalpy). The turbocharger turbine converts the exhaust gas enthalpy into the mechanical energy which is then delivered directly to the charger (blower).

In each measurement set, the exhaust gas temperature before the turbocharger turbine increases with the increase in the fuel mass flow, Figure 9. In the measurement Set 1 and at 1500 rpm, the temperature of the exhaust gas before the turbine ranges from 317.18 °C at the lowest observed fuel mass flow, up to 609.33 °C at the highest observed fuel mass flow. In the measurement Set 2 and at 2400 rpm, the exhaust gas temperature before the turbine ranges from 385.83 °C up to 620.09 °C.

For the same fuel mass flow, significantly higher exhaust gas temperature before turbocharger turbine can be seen in the measurement Set 1 at a lower engine rotational speed, Figure 9. Therefore, in measurement Set 1, at the same fuel mass flow, the higher heat content is available for the turbine operation than in Set 2.

Comparing the temperatures of the exhaust gas before (Figure 9) and after (Figure 10) the turbocharger turbine, it is evident that they have almost identical trends. This fact points to the stability of the turbocharger turbine operation without any noticeable oscillations which would be primarily visible in the uneven change of exhaust gas temperatures before and after the turbine.

Identical to the exhaust gas temperature before the turbine, in each measurement set the exhaust gas temperature after the turbine increases with the increase in the fuel mass flow, Figure 10. In the measurement Set 1, the exhaust gas temperature after the turbine ranges from 285.57 °C at the lowest fuel mass flow up to 536.38 °C at the highest fuel mass flow. In the measurement Set 2, the exhaust gas temperature after the turbine ranges from 316.12 °C to 479.33 °C.

The maximum exhaust gas temperature after the turbine in Set 1 is 72.95 °C lower than the maximum temperature before the turbine, while the maximum exhaust gas temperature after the turbine in the measurement Set 2 is 140.76 °C lower than the maximum temperature before the turbine.

6 Conclusion

The paper aims to present the main operating parameters change for a high speed turbocharged direct injection diesel engine MAN D0826 LOH15 during the fuel mass flow variation. The analysis has been based on two measurement sets at two different engine rotational speeds (1500 rpm and 2400 rpm).

According to the measurement results, the following engine main operating parameters have been calculated: engine torque, effective power, excess air ratio, specific effective fuel consumption and heat released per engine process. During the variation in the fuel mass flow, for both engine measurement sets, the obtained engine torque has been in the range 225.86 Nm to 691.52 Nm, while the engine effective power has been in the range 41.93 kW to 145.56 kW. It is important to notice that there is no observed operating point in which the engine peak effective power of 160 kW has been obtained. In the same analyzed measurement sets, the air excess ratio continuously decreases during the increase in the fuel mass flow. The highest air excess ratio amounts to 2.87 in the measurement Set 2, while the lowest air excess ratio amounts to 1.46 in the measurement Set 1. The specific effective fuel consumption firstly decreases followed by a slight increase after, during the increase in the fuel mass flow. The lowest obtained specific fuel consumption has been at 214.96 g/kWh in the measurement Set 1. The measurement Set 1 has shown a wider range of heat released per engine process in comparison with the measurement Set 2. In Set 1, the heat released per engine process amounts from 4.44 kJ/proc. up to 10.64 kJ/proc.

Additionally measured engine operating parameters, which are not presented as a part of any measurement set, have presented engine operating parameters necessary for detailed engine simulations. The lubrication oil temperature does not exceed 113 °C in any of the observed engine operation points, what is far below the limit values prescribed by the manufacturer. The same trend of exhaust gas temperatures before and after the turbocharger turbine provides information about the satisfactory turbine operation regimes. Those two temperatures are the essential measurement data for a detailed analysis of the exhaust gas turbine operation and turbocharging process as a whole.

The diesel engine analysis has been performed with a standard diesel fuel. In future research, it will be interesting to compare the same operating parameters with those obtained when the engine uses alternative fuels or its blends with standard diesel fuel.

Acknowledgments

The authors express their thankful regards to the whole team at the Laboratory for Internal Combustion Engines and Electromobility (LICeM), at the Faculty of Mechanical Engineering, University of Ljubljana, Slovenia. This work has been supported by the University of Rijeka (contract no. 13.09.1.1.05) and the Croatian Science Foundation-project 8722.

References

[1] Martyr, A. J., Plint, M. A.: *Engine Testing – Theory and Practice*, Third edition, Butterworth-Heinemann, Elsevier Ltd., 2007.

[2] Merker, G. P., Schwarz, C., Teichmann, R.: *Combustion Engines Development – Mixture Formation, Combustion, Emis-*

sions and Simulation, Springer-Verlag, Berlin, Heidelberg, 2012. (doi: 10.1007/978-3-642-14094-5)

[3] Mollenhauer, K., Tschoeke, H.: *Handbook of Diesel Engines*, Springer-Verlag, Berlin, Heidelberg, 2010. (doi: 10.1007/978-3-540-89083-6)

[4] Reif, K.: *Diesel Engine Management – Systems and Components*, Springer Fachmedien, Wiesbaden, 2014. (doi: 10.1007/978-3-658-03981-3)

[5] Dempsey, P.: *Troubleshooting and Repairing Diesel Engines*, Fourth Edition, The McGraw-Hill Companies, Inc., 2008. (doi: 10.1036/0071493719)

[6] Lakshminarayanan, P. A., Aghav, Y. V.: *Modelling Diesel Combustion*, Springer Science, 2010. (doi: 10.1007/978-90-481-3885-2)

[7] Medica, V.: *Simulation of turbocharged diesel engine driving electrical generator under dynamic working conditions*, Doctoral Thesis, Rijeka, University of Rijeka, 1988.

[8] Murphy, A. J., Norman, A. J., Pazouki, K., Trodden, D. G.: *Thermodynamic simulation for the investigation of marine Diesel engines*, Ocean Engineering, 102, pp. 117–128, 2015. (doi: 10.1016/j.oceaneng.2015.04.004)

[9] Rakopoulos, C.D., Rakopoulos, D.C., Giakoumis, E.G., Kyritsis, D.C.: *Validation and sensitivity analysis of a two zone Diesel engine model for combustion and emissions prediction*, Energy Conversion and Management, 45, pp. 1471–1495, 2004. (doi: 10.1016/j.enconman.2003.09.012)

[10] Škifić, N.: *Influence analysis of engine equipment parameters on diesel engine characteristics*, Doctoral Thesis, Rijeka, University of Rijeka, 2003.

[11] Mrzljak, V., Medica, V., Bukovac, O.: *Volume agglomeration process in quasi-dimensional direct injection diesel engine numerical model*, Energy, 115, pp. 658–667, 2016. (doi: 10.1016/j.energy.2016.09.055)

[12] Mrzljak, V., Medica, V., Bukovac, O.: *Simulation of a Two-Stroke Slow Speed Diesel Engine Using a Quasi-Dimensional Model*, Transactions of Famena, 2, pp. 35–44, 2016. (doi: 10.21278/TOF.40203)

[13] Rakopoulos, C. D., Giakoumis, E. G.: *Diesel Engine Transient Operation – Principles of Operation and Simulation Analysis*, Springer-Verlag London, 2009. (doi: 10.1007/978-1-84882-375-4)

[14] Meloni, R., Naso, V.: *An insight into the effect of advanced injection strategies on pollutant emissions of a heavy-duty diesel engine*, Energies, 6, pp. 4331–4351, 2013. (doi: 10.3390/en6094331)

[15] Huang, M., Gowdagiri, S., Cesari, X. M., Oehlschlaeger, M. A.: *Diesel engine CFD simulations: Influence of fuel variability on ignition delay*, Fuel, 181, pp. 170–177, 2016. (doi: 10.1016/j.fuel.2016.04.137)

[16] Ramesh, N., Mallikarjuna, J. M.: *Low Temperature Combustion Strategy in an Off-Highway Diesel Engine – Experimental and CFD study*, Applied Thermal Engineering, 124, pp. 844–854, 2017. (doi: 10.1016/j.applthermaleng.2017.06.078)

[17] Jamrozik, A.: *The effect of the alcohol content in the fuel mixture on the performance and emissions of a direct injection diesel engine fueled with diesel-methanol and diesel-ethanol blends*, Energy Conversion and Management, 148, pp. 461–476, 2017. (doi: 10.1016/j.enconman.2017.06.030)

[18] Hoseini, S.S., Najafi, G., Ghobadian, B., Rahimi, A., Yusaf, T., Mamat, R., Sidik, N.A.C., Azmi, W.H.: *Effects of biodiesel fuel obtained from Salvia Macrosiphon oil (ultrasonic-assisted) on performance and emissions of diesel engine*, Energy, 131, pp. 289–296, 2017. (doi: 10.1016/j.energy.2017.04.150)

[19] Othman, M.F., Adam, A., Najafi, G., Mamat, R.: *Green fuel as alternative fuel for diesel engine: A review*, Renewable and Sustainable Energy Reviews, 80, pp. 694–709, 2017. (doi: 10.1016/j.rser.2017.05.140)

[20] Tamilselvan, P., Nallusamy, N., Rajkumar, S.: *A comprehensive review on performance, combustion and emission characteristics of biodiesel fuelled diesel engines*, Renewable and Sustainable Energy Reviews, 79, p. 1134–1159, 2017. (doi:10.1016/j.rser.2017.05.176)

[21] Park, S., Kim, Y., Woo, S., Lee, K.: *Optimization and calibration strategy using design of experiment for a diesel engine*, Applied Thermal Engineering, 123, pp. 917–928, 2017. (doi: 10.1016/j.applthermaleng.2017.05.171)

[22] Park, S., Cho, J., Park, J., Song, S.: *Numerical study of the performance and NOx emission of a diesel-methanol dual-fuel engine using multi-objective Pareto optimization*, Energy, 124, pp. 272–283, 2017. (doi: 10.1016/j.energy.2017.02.029)

[23] Kumar, B.R., Saravanan, S., Sethuramasamyraja, B., Rana, D.: *Screening oxygenates for favorable NOx/smoke trade-off in a DI diesel engine using multi response optimization*, Fuel, 199, pp. 670–683, 2017. (doi: 10.1016/j.fuel.2017.03.041)

[24] Navid, A., Khalilarya, S., Taghavifar, H.: *Comparing multi-objective non-evolutionary NLPQL and evolutionary genetic algorithm optimization of a DI diesel engine: DoE estimation and creating surrogate model*, Energy Conversion and Management, 126, pp. 385–399, 2016. (doi: 10.1016/j.enconman.2016.08.014)

[25] Channapattana, S.V., Pawar, A.A., Kamble, P.G.: *Optimisation of operating parameters of DI-CI engine fueled with second generation Bio-fuel and development of ANN based prediction model*, Applied Energy, 187, pp. 84–95, 2017. (doi: 10.1016/j.apenergy.2016.11.030)